Human corneal fibroblast migration and ECM synthesis during stromal repair: Role played by PDGF-BB, bFGF, and TGFβ1

(HCFs migration and ECM synthesis during stromal repair: GFs effects)

Patricia Gallego-Muñoz[1], Lucía Ibares-Frías[1, 2], José A. Garrote[3], María Cruz Valsero-Blanco[4], Roberto Cantalapiedra-Rodríguez[1], Jesús Merayo-Lloves[5], M. Carmen Martínez-García[1]

[1]Departamento de Biología Celular, Histología y Farmacología. Facultad de Medicina. Grupo de Investigación Reconocido: Técnicas Ópticas para el Diagnóstico. Universidad de Valladolid, Valladolid, Spain.

[2]Servicio de Oftalmología, Hospital Clínico Universitario de Valladolid, Valladolid, Spain.

[3]Servicio de Análisis Clínicos. Laboratorio de Genética, Hospital Universitario Rio Hortega de Valladolid, Valladolid, Spain.

[4]Departamento de Estadística, Facultad de Ciencias, Universidad de Valladolid, Valladolid, Spain.

[5]Instituto Oftalmológico Fernández-Vega. Universidad de Oviedo, Oviedo, Spain.

Grant information: Patricia Gallego-Muñoz was funded by the Regional Government of Castilla y León FPI Programme (co-funded by the European Social Fund), Spain.

Corresponding author: Dr. M. Carmen Martínez García. Departamento de Biología Celular, Histología y Farmacología. Facultad de Medicina. Universidad de Valladolid. C/ Ramón y Cajal 7, 47005, Valladolid, Spain.

E-mail address: mariacarmen.martinez.garcia@uva.es

Phone: +34983184777

The authors have no commercial relationship with any of the materials mentioned in the article.

This article has been accepted for publication and undergone full peer review but has not been through the copyediting, typesetting, pagination and proofreading process which may lead to differences between this version and the Version of Record. Please cite this article as doi: 10.1002/term.2360

Abstract

The development of treatments that modulate corneal wound healing to avoid fibrosis during tissue repair is important for the restoration of corneal transparency after an injury. To date, few studies have studied the influence of growth factors (GFs) on human corneal fibroblast (HCF) expression of extracellular matrix (ECM) proteins such as collagen types I and III, proteoglycans such as perlecan, or proteins implicated in cellular migration such as α5β1-integrin and syndecan-4. Using in vitro HCFs, we developed a mechanical wound model to study the influence of the GFs basic fibroblast growth factor (bFGF), platelet-derived growth factor (PDGF-BB), and transforming growth factor beta 1 (TGFβ1) on ECM protein production and cellular migration. Our results show that mechanical wounding provokes the autocrine release of bFGF and TGFβ1 at different time points during the wound closure. The HCF response to PDGF-BB was a rapid closure due to fast cellular migration associated with a high focal adhesion replacement and a high expression of collagen and proteoglycans, producing a non-fibrotic healing. bFGF stimulated non-fibrotic ECM production and limited the migration process. Finally, TGFβ1 induced expression of the fibrotic markers collagen type III and α5β1 integrin, and it inhibited cellular migration due to the formation of focal adhesions with a low turnover rate.

The novel in vitro HCF mechanical wound model can be used to understand the role played by GFs in human corneal repair. The model can also be used to test the effects of different treatments aimed at improving the healing process.

Keywords: corneal stroma repair, migration, ECM synthesis, TGFβ1, PDGF-BB, bFGF, human corneal fibroblasts.

1. Introduction

The cornea is the most external part of the eye. It has two essential properties: a curved shape and transparency. Associated with these two properties are two fundamental functions: refraction and light transmission to the retina. Histologically, the cornea consists of an epithelium, stroma, and endothelium. The thickest part of the cornea is the stroma, which is mainly composed of an extracellular matrix (ECM) comprised mostly of fibrillar collagen types I and V (Birk et al., 1986). The transparency of the cornea depends upon the parallel alignment of the lamellae and the uniform spacing between them. Proteoglycans play regulatory roles in collagen fibril diameter and fibril organization by maintaining the interfibrillar distance in the collagen network (Funderburgh et al., 2001). Distributed among the collagen fibers are keratocytes, a population of quiescent, neural crest-derived mesenchymal cells that have a compact dendritic morphology. This morphology ensures the interconnection of the keratocytes with the three dimensional network of the ECM (Hahnel et al., 2000).

The transparency of the cornea can be compromised by trauma, inflammation, and burns. Regeneration of the cornea involves proliferation, differentiation, migration of the keratocytes, and synthesis of new ECM. The quiescent keratocytes flanking the wound are stimulated to acquire the “activated” phenotypes: fibroblasts and myofibroblasts (West-Mays and Dwivedi, 2006).

The activated phenotypes are dependent on specific environmental signals such as growth factors (GFs). An important feature that has a significant impact on corneal repair and makes the cornea different from the other tissues is its avascular nature (Fini, 1999). Consequently, the regulatory GFs must come from other sources

such as the tear, epithelium, stroma, or inflammatory cells (Imanishi et al., 2000; Wilson et al., 2001), all of which play a key role in wound repair responses.

Transforming growth factor β1 (TGFβ1), basic fibroblast growth factor (bFGF), and platelet derived growth factor BB-isoform (PDGF-BB) are examples of GFs involved in corneal wound healing (Etheredge et al., 2009; Imanishi et al., 2000). Keratocytes can be activated in vitro by these GFs in a similar way to the in vivo keratocyte response to injury (Etheredge et al., 2009; Kim et al., 2010; Kim et al., 1999; Long et al., 2000; Maltseva et al., 2001).

The fibroblasts proliferate and develop stress fibers to migrate into the wound area so as to repopulate and close the wound. Some fibroblasts that reach the wound become myofibroblasts. These cells deposit provisional ECM and contract the wound. Excessive stromal myofibroblast generation and the resulting disorganized ECM synthesis after the wound healing process are associated with permanent corneal opacity (Torricelli et al., 2013). The development of a corneal opacity during wound healing is also affected by the presence of a regenerated basal membrane that can limit the access of epithelium-derived growth factors, such as TGFβ1, that are responsible for myofibroblast development and persistence (Singh et al., 2012).

The new matrix secreted by activated phenotypes during the healing process modulates important aspects of cell behavior such as adhesion, migration, and differentiation. The matrix also affects GF activity and bioavailability, and it acts as the substratum for cell migration. Fibroblasts and myofibroblasts have transmembrane proteins that recognize ECM and interact with the cytoskeleton, for example, integrins and syndecans. The new ECM contains fibronectin, tenascin and collagen type III (Col III), a fibrillar collagen present in fetal and wounded corneas,

but not usually detected in normal adult stroma (Chen et al., 2000). The proteoglycan component of the new ECM includes the heparan sulfate proteoglycans (PGs) perlecan and syndecan-4 (SDC4). These PGs regulate collagen interfibril order and hydration, both of which are essential to obtain the necessary transparency (Rawe et al., 1994). Perlecan is present at low levels in the normal stroma and increases upon injury (Hassell et al., 1983; Sundarraj et al., 1998). SDC4, a transmembrane PG, is localized in focal adhesion areas of adherent cells such as fibroblasts (Woods and Couchman, 1994). This protein has high binding capacity for different extracellular ligands and plays important roles in cellular adhesion, migration, and proliferation (Carey, 1997).

Cell migration requires integrins that link cytoskeletal actin at focal adhesions of the migrating cells to the substratum. During wound healing, the focal adhesions are dynamic and transmit mechanical and biochemical signals between the migrating cells and the substratum. Integrins regulate the capacity of keratocytes, fibroblasts, and myofibroblasts to assemble and maintain the collagen/PG rich matrix to limit corneal scarring (Stepp, 2006). In normal corneal stroma, α5β1 integrin, the high-affinity fibronectin receptor, is not expressed, although it does appear in regions of scar formation in human corneas (Carter, 2009). The levels of α5β1 integrin are high in fibrillar adhesions that arise from focal adhesions in migrating cells (Le Clainche and Carlier, 2008).

The role played by GFs on cellular response has often been studied. However, the relationship between GF signaling and ECM synthesis and secretion, is not well understood. Herein, we report the use of cultured human corneal fibroblasts (HCFs) to study the effects of specific recombinant GFs, TGFβ1, bFGF, and PDGF-BB, on ECM development and migration in corneal wound repair. For this purpose, we

developed an in vitro model in which the cultured HCFs were wounded by a standardized mechanical scratch, and the wound healing response during closure was assessed with and without GF supplementation.

2. Material and methods

2.1. Culture of HCFs

Six human corneal rims from transplanted corneas were obtained from the Principado de Asturias Eye Bank (Oviedo, Spain). All research adhered to the tenets of the Declaration of Helsinki. After removal of the epithelium and endothelium using a sterile technique under a dissecting microscope, the keratocytes were released from the stroma by incubation with collagenase type II (2 mg/mL; Gibco, Carlsbad, CA, USA) as previously described (Bernstein et al., 2004). Cell number and viability were determined using trypan blue exclusion. The culture medium was a 1:1 mixture of Dulbecco´s modified Eagle´s medium and Ham´s nutrient mixture F-12 (DMEM-F12, Gibco) supplemented with 10% fetal bovine serum (FBS; Sigma; St. Louis, MO, USA) and a 1% antibiotic-antimycotic solution (Sigma). Cells were seeded in 35-mm plates (2 X 10^5 cells/2 mL/plate) and maintained at 37ºC in 5% CO_2 until grown to near confluence. The culture medium was changed every other day, and the cells were amplified by culturing for seven passages. All experiments were carried out with cells on the seventh passage (7P).

2.2. Wound formation and GF supplementation

HCFs were seeded onto 35-mm plates (2 X 10^5 cells/2 mL/plate). To reduce serum-induced activation and to study the effects of each GF individually during wound closure, serum-free medium (SFM) was added three days after the 7P passage, when the cells reached 90% confluence. After a further three days of culture in SFM, the tip of a disposable 10 µL pipette was used to make a linear wound in the center of the plate. The wound length and width were 35 mm and 0.768 mm respectively, creating a wound area of 26.8 mm^2. The effects of different GFs on wound closure were assessed on Days 1, 4, 7, 10, and 15.

Immediately after making the wound, the medium was replaced with fresh SFM alone (control) or supplemented with either 10 ng/ml TGFβ1, 10 ng/ml bFGF, or 20 ng/ml PDGF-BB, all from Gibco. Unwounded cultures were not included because treated cells detached from confluent cultures. Optimal GF concentrations were determined from preliminary dose-response experiments. The concentrations used for further experiments were the lowest that gave a maximal and non-toxic response.

2.3. GFs detection in the culture media

On Days 1, 4, and 7 after making the wounds, the cell culture medium was collected to assay the secretion of TGFβ1, bFGF, and PDGF-BB by enzyme-linked immunosorbent assay (ELISA). We used the multispecies TGFβ1 ELISA kit (KAC1688, Invitrogen, Carlsbad, CA, USA), the human FGF basic ELISA kit (KHG0021, Invitrogen), and the human PDGF-BB ELISA kit (DBB00, R&D Systems, Minneapolis, MN, USA) following the instructions provided by each kit. For cases in which the incubation media were supplemented with a specific GF, only the detection of the other two GFs was studied. All samples were analyzed in duplicate,

and GF concentrations (pg/mL) were determined as the mean from 2 or 3 samples for each treatment.

2.4. Wound closure

Wound closure was assessed under a Nikon Eclipse TE300 inverted microscope with a Nikon DXM1200 digital camera incorporated (Nikon Instruments, Inc.; Melville, NY, USA) taking microphotographs at different time points. In addition, three plates per group were fixed and stained with Giemsa´s solution (Giemsa´s azur eosin methylene blue solution, Merck Kga, Darmstadt, Germany), visualized with light microscopy (BX41 Carl Zeiss, Oberkochen, Germany) and microphotographs were taken with an Olympus DP20 digital camera incorporated (Olympus Optical Co, Tokyo, Japan). Wound dimensions were measured on post-wounding Days 1, 4, 10, and 15 with Soft Cell^{A} Imaging Software for Life Science Microscopy (Olympus Optical Co). Each measurement was obtained from 5 or 6 observations of the wound width taken along the 35-mm length of the wound.

2.5. RNA isolation, cDNA synthesis, and qRT-PCR

On post-wound Day 7, total RNA from the HCFs was extracted with Trizol LS Reagent (Applied Biosystems [ABI], Life Technologies, Foster City, CA, USA) following the manufacturer´s protocol. This time point was chosen because it was an intermediate time in which the wounds were still closing. Cells were harvested from four plates of each treatment. In three independent experiments, the RNA obtained was reverse-transcribed to cDNA using the high-capacity cDNA reverse transcription kit with RNAse inhibitor (ABI), following the vendor´s instructions. Quantitative real-time PCR (qRT-PCR) was conducted on a Light Cycler 480 (Roche, Madrid, Spain)

using the ABI TaqMan Gene Expression Master Mix and ABI TaqMan gene expression assays for the following genes: perlecan, Hs00194179_m1; SDC4, Hs00161617_m1; keratocan, Hs00559942_m1; α5 integrin subunit, Hs01547673_m1; β1 integrin subunit, Hs00559595_m1; and actin beta (ACTB), Hs 9999903_m1 as the endogenous control. Reactions were run in duplicate in total volumes of 10 μL. For the internal standardization curve, gene expression for ACTB, SDC4, perlecan, and α5 and β1 integrin subunits was obtained using mRNA isolated from normal human dermal fibroblasts (NHDF pellet, C-14030; PromoCell; Barcelona, Spain) that strongly express each marker (calibrator). Calibrator expression for keratocan was obtained from mRNA expression in human corneal stromal rims. Relative transcript levels were calculated by normalizing threshold cycle (Ct) values to the endogenous control ACTB. All sample results were expressed relative to SFM samples that were normalized to one.

2.6. Western Blot

On post-wound Day 7, total protein from the HCFs were extracted with radio-immunoprecipitation assay (RIPA) buffer (Santa Cruz Biotechnology, Santa Cruz, CA, USA). Cells were harvested from two plates of each treatment. Sample lysates were resolved equally on a denaturing 10% or 6% sodium dodecyl sulfate-polyacrylamide gel and later transferred to polyvinylidene difluoride (PVDF) membranes (Immobilon-p, IPVH00010; Millipore, Madrid, Spain). Membranes were incubated with the primary antibodies to collagen type I (Col I, 234167, Millipore), Col III (sc-sc-8780-R), perlecan (sc-377219), and SDC4 (sc-15350), all from Santa Cruz Biotechnology, except Col I, followed by HRP-conjugated secondary antibodies (NA9340 or NA9310; VWR International, Ltd., Radnor, PA, USA). Immunoreactive

bands were detected by enhanced chemiluminescence (Pierce, Rockford, IL, USA). For protein normalization, blots were stripped and reproved with primary antibody to ACTB (βactin, sc-69879; Santa Cruz). Densitometry was performed using Quantity One Software (Bio-Rad, Hercules, CA, USA). Results were expressed relative to SFM samples that were normalized to one. Values were determined as the means from two independent experiments.

2.7. Immunofluorescence staining

Immunocytochemistry was performed on HCFs seeded onto 35-mm culture plates with cover-slips at the bottom. Four days after the wounds were made, the cells were fixed in 1% paraformaldehyde, permeabilized in pre-chilled 0.1% TX-100 (Sigma) and blocked in 1% bovine serum albumin in PBS (PBSA) plus 3% goat serum, followed by incubation with primary antibodies to α5β1 integrin (MAB1969; Millipore) and SDC4 (Santa Cruz Biotechnology). After rinsing, secondary antibodies Alexa Fluor 488 and 594 (Life Technologies) diluted in PBSA were applied. Imaging of cell cultures was performed with a Leica confocal microscope and Leica Application Suite Advanced software (Leica TSC SP, Wetzlar, Germany). All samples were examined with 40x lens. All images were taken under the same conditions including laser intensity, contrast, brightness, and pinhole size to compare the labels. Experiments were performed at least three times, and each yielded similar results.

2.8. Statistics

Means ± standard deviations, statistical analyses by multifactor analysis of variance (ANOVA), and the Kruskal-Wallis test or Mood´s median test (depending on Levene´s test for homogeneity of variances) were performed on Statgraphics Centurion XVI (StatPoint Technologies, Inc.; Warrenton, VA, USA). $P < 0.05$ was considered to be statistically significant.

3. Results

3.1. Detection of GFs in the culture media

First, we demonstrated that disruption of HCF cell junctions by the wound causes the cells themselves to release growth factors. One day after wounding, only bFGF was detected in the culture media. The highest level was recovered in the supernatant of cells cultured in SFM, followed by cells cultured in PDGF-BB, although the difference between the two treatments was not significant (Fig. 1A). Both treatments resulted in significantly higher levels of bFGF than in cultures treated with TGFβ1, where it was undetectable (Fig. 1A). On Day 4, none of the GFs studied was detected, and at Day 7, only TGFβ1 was detected (Fig. 1B). The levels of TGFβ1 present in PDGF-BB-treated cells were significantly higher than in SFM- and bFGF-treated cells, both of which had similar levels of this GF.

3.2. Wound closure

Differences in wound closure rates were apparent among groups over time depending on the GF added to the media (Fig. 2). These differences were statistically significant ($p<0.001$) except between PDGF-BB- and bFGF-treated wounds (Table 1). The pattern of healing was similar for both PDGF-BB- and bFGF-treated wounds, and closure was completed at Day 10 (Fig. 2I and 2K). At that time, wound closure with TGFβ1 was smaller than SFM-treated wounds ($p<0.01$). While the wound closure process with SFM was slower than PDGF-BB- and bFGF-treated cells, it proceeded to completion by Day 15 (Fig. 2D). For cultures treated with TGFβ1, wound closure was not completed by the end of the study (Fig. 2G).

3.3. Keratocan expression

Expression of keratocan mRNA was not detected in any of the samples (data not shown).

3.4. Relative abundance of Cols I and III

In all groups studied, the relative abundance of Col I increased with regard to SFM. The increases were significantly higher in TGFβ1-treated cells (Fig. 3A). As in the results for Col I, in TGFβ1- and PDGF-BB-treated cells, the relative abundance of Col III increased with regard to SFM (Fig. 3B) although only the results for PDGF-BB-treated cells were significantly higher than the SFM group. In contrast, in bFGF-treated cells, the levels were smaller than SFM, although the differences between the two groups were not significant.

3.5. α5 and β1 integrin subunits mRNA expression and protein localization

The expression of both α5 and β1-integrin subunits was up-regulated in TGFβ1- and PDGF-BB-treated cells, and down-regulated in bFGF-treated cells (Fig. 4). α5β1 integrin protein localization in the cells differed depending on treatment (Fig. 5A-D). In SFM cells, it was distributed throughout the cytoplasm without any unique location (Fig. 5A). In contrast, the highest levels of this protein were observed in TGFβ1-treated cells, where it was mainly localized at the trailing edge of the cells and around the nuclei (Fig. 5B; arrowheads), making up fibrillar adhesions. In PDGF-BB-treated cells, the integrin was mainly localized at the leading edge of the cells forming longer focal complexes (Fig. 5C; arrowheads). Finally, bFGF-treated cells showed very low levels of α5β1-integrin (Fig. 5D).

3.6. SDC4 mRNA expression, relative abundance, and localization

Expression of SDC4 proteoglycan mRNA was up-regulated in bFGF- and PDGF-BB-treated HCFs and down-regulated in TGFβ1-treated cells (Fig. 6A). Compared to HCFs treated with TGFβ1 and PDGF-BB, levels of SDC4 were significantly lower in bFGF-treated cells ($p < 0.05$, Fig. 6B-C). Among the three other treatment groups, there were no significant differences in the levels of this proteoglycan ($p > 0.05$).

In SFM-treated cells, this proteoglycan was homogenously distributed in the cytoplasm (Fig. 5A´), showing very low co-localization with the integrin (Fig. 5A´´; arrows). In contrast, in TGFβ1-treated cells, the SDC4 was localized mainly in the less motile regions of the wounded cultures, such as around the nuclei (Fig. 5B´; arrowheads) where it co-localized with the α5β1 integrin (Fig. 5B´´; arrows). These cells had the highest levels of the SDC4, which also appeared in the filopodia at the leading edge of the cells as dot-like structures (Fig. 5B´; asterisks). In PDGF-

BB-treated cells, the SDC4 levels were lower than in TGFβ1-treated cells (Fig. 5C´) although it co-localized with the integrin mainly in the trailing edge of the migrating cells (Fig. 5C´´; arrows). Finally, the relative abundance of SDC4 in bFGF-treated cells was low (Fig. 6B). However higher expression was present in the adhesion complexes at the leading edge (Fig. 5D´; arrowheads), but with very low integrin co-localization (Fig. 5D´´; arrows) as shown by immunocytochemistry.

3.7. Perlecan mRNA expression and relative protein abundance

Compared to SFM cultures, the relative mRNA expression of perlecan increased in PDGF-BB- and bFGF-treated cells (Fig. 6D). In contrast, the expression was down-regulated in TGFβ1-treated cultures. The relative abundance of perlecan protein was similar among the HCFs treated with SFM, TGFβ1, and bFGF ($p > 0.05$, Fig. 6C and 6E). However, perlecan was present at significantly higher levels in cells treated with PDGF-BB ($p < 0.05$).

4. Discussion

Developing treatments that modulate corneal wound closure and avoid fibrosis during tissue regeneration are important goals. Growth factors play important roles in this process. Therefore, understanding the specific action of each factor helps develop new therapies that utilize these agents to avoid the development of corneal opacity.

TGFβ, PDGF, and FGF have crucial functions in modulating myofibroblast differentiation (Maltseva et al., 2001; Singh et al., 2011). While TGFβ1 and bFGF are produced by corneal epithelial and stromal cells (Imanishi et al., 2000; Kay et al., 1998; Wilson et al., 1994), PDGF-BB is only produced by the epithelium (Kim et al., 1999; Wilson et al., 2001).

There are many in vivo and in vitro reports designed to gain a better understanding of the corneal response to GFs (Etheredge et al., 2009; Hassell et al., 1992; Kim et al., 2010; Maltseva et al., 2001; Petroll et al., 2012; Song et al., 2002; Tuli et al., 2006). However, most have not been carried out with human cells or lack a stimulus such as a wound. More recent studies on cultured human corneal fibroblasts have shown that the cellular responses to a mechanically-made wound are different from the responses to different treatments observed without making a wound (Anitua et al., 2015; Sloniecka et al., 2016). According to this, in the present study, we inflicted wounds with adequate dimensions on HCFs cultures to study the migration and ECM synthesis during the wound closure, and also, to study the influence of three of the main GFs involved in stroma repair (bFGF, PDGF-BB and TGFβ1) on both key processes.

Due to the stimulation that our injury provokes, cells release GFs in an autocrine manner. Secretion of bFGF occurred very soon after wounding (24 h), while TGFβ1 secretion was detected later (Day 7). bFGF secretion was not detected after TGFβ1 supplementation, while PDGF-BB supplementation significantly increased secretion of TGFβ1.

As in previous studies (Kim et al., 1999; Wilson et al., 2001), we did not detect PDGF-BB secretion in any case. As we found, prior studies (Song et al., 2002; Wang et al., 2011) showed that corneal stromal fibroblasts produce both TGFβ1 and bFGF. However, Song et al., (2002) found a different pattern of bFGF and TGFβ1 secretion. They concluded that TGFβ1 mediates the early phases of wound repair whereas bFGF plays a role in modulating later responses. Such contradictory results are possibly due the fact that the wounds made by Song et al. were smaller than ours and were observed for no more than 24 hours.

Around the injured zone, keratocytes are activated to repopulate the acellular zone. Several simultaneous events are needed to refill the area: proliferation, migration, and synthesis and deposition of a new matrix. The extracellular matrix synthesized by fibroblasts and myofibroblasts provides support for cells and their migration. This ECM is basically made up of Col I (Michelacci, 2003), although Col III expression increases during wound healing, and is considered a marker of repair matrix synthesis. When Col III is secreted in excess, it is also considered as a sign of fibrosis (Galiacy et al., 2011; Michelacci, 2003). As our results show, TGFβ1 supplementation significantly increased the levels of Cols I and III. This result is indicative of the synthesis of a fibrotic matrix. PDGF-BB treatment produced intermediate levels whereas bFGF supplementation did not affect the levels of either collagen type.

In our wound repair model, wound closure was very quick in cultures supplemented with PDGF-BB and with bFGF, but very slow in SFM cultures and even slower in TGFβ1-treated cultures, which remained open at Day 15. To search for an explanation for these results, we studied the cellular migration process in which the SDC4 and the α5β1 integrin are directly involved (Bass et al., 2007; Brooks et al., 2012). In the leading edge of the migrating cells, actin assembly induces development of lamellipodia and filopodia (Zaidel-Bar et al., 2003) . In these structures, the cells form adhesions that connect the extracellular matrix to the actin cytoskeleton and anchor the lamellipodia, exerting traction within the cell body. After that, the cell must retract its trailing edge via disassembly of adhesions at the rear (Zaidel-Bar et al., 2003). The highly dynamic structures formed during adhesion turnover at the leading edge are focal complexes. When focal complexes do not disassemble, they mature into focal structures (fibrillar adhesions) which are more stable and longer lasting than adhesion complexes, with slow turnover located at the cell periphery and more centrally. These structures contain high levels of α5β1 integrin that is implicated in migratory activity (Le Clainche and Carlier, 2008). TGFβ1 treatment induced high levels of this integrin that co-localized with the SDC4, mainly on the trailing edge of the cells four days after wounding. The association of integrin with SDC4 could have set up strong focal and fibrillar adhesions that prevented the migration process. Cultures treated with TGFβ1 had the highest levels of the SDC4 protein at Day 7 and the lowest levels of the SDC4 mRNA at the same time, suggesting there is a very low turnover of this protein. This PG increases after wounding and induces the cells located at the wound edges to increase adhesion and contract the wound (Couchman and Woods, 1999). Taken together, our data show that cultured HCFs stimulated with TGFβ1 have low rates of migration, which is

consistent with the fact that the wounds remained open after 15 days of culture. These results are supported because the proliferative rate induced by TGFβ1 treatment is high during the closure (data not shown). Thus, in spite of the fact that TGFβ1 induced a high rate of proliferation, closure of the wounds was slow and incomplete after 15 days of culture.

In contrast with TGFβ1, PDGF-BB treatment resulted in lower levels of α5β1 integrin, which was localized by immunocytochemistry mainly at the leading edge of the migrating cells. This contrasts with the highest relative expression of α5 and β1 integrin subunit mRNAs at Day 7, which suggests a high turnover rate. At the same time, these cells had the highest SDC4 mRNA expression and a high relative abundance of the protein. Hence, these dynamic adhesions could enable the high rate of migration observed in PDGF-BB-treated cells. Thus, the high proliferation rate soon after wounding (data not shown) and the rapid migration rate induced by PDGF-BB treatment can explain, at least in part, the rapid wound closure, completed by Day 10, induced by this GF.

bFGF treatment induced a quick wound closure. This confirms that bFGF increases proliferation as previously described (Boilly et al., 2000; Song et al., 2002) and as we documented in other experiments (data not shown). Nevertheless, bFGF did not favor rapid migration as indicated by the lowest levels of α5β1 integrin and SDC4 protein.

PG expression also plays a significant role during wound healing. The PGs SDC4 and perlecan, both of which increase upon corneal injury (Hassell et al., 1983; Sundarraj et al., 1998), are markers of the non-fibrotic repair phenotype (Carey, 1997; Mongiat et al., 2000), and both are important for maintaining corneal integrity. Previous studies have described how perlecan production by stromal cells might contribute to rapid basal membrane regeneration after an injury (Maguen et al., 2008; Torricelli et al., 2015). During wound closure in cultures treated with PDGF-BB and bFGF, expression of perlecan mRNA was up-regulated compared to SFM-treated control wounds. PDGF-BB treatment also induced a significant increase in the relative abundance of perlecan protein. Thus the stromal production might contribute to the rapid recovery of the epithelial basal membrane and, as a result, lower myofibroblast development, as recently described (Torricelli et al., 2015). In the present study, the expression levels of these proteoglycan mRNAs were down-regulated when cultures were treated with TGFβ1.

5. Conclusions

The principal findings of this study can be summarized as follows: (1) bFGF was secreted in an autocrine manner soon after the wounding of cultured HCFs. It promoted synthesis of a non-fibrotic ECM and limited the cellular migration process. (2) PDGF-BB induced an increase in the autocrine secretion of TGFβ1. It also induced high cellular motility and synthesis of non-fibrotic matrix PGs. This is consistent with promoting non-fibrotic wound healing. (3) TGFβ1 was secreted later in the wound closure process, and adding it to the culture medium reduced bFGF secretion to undetectable levels. It also significantly increased the relative abundance of Col I and III and greatly reduced cellular motility.

The cellular modulation induced by the GFs tested here has considerable biological and clinical relevance. The in vitro HCFs provide a good model for studying the mechanism(s) by which defective wound healing occurs and for stimulating or inhibiting certain wound healing stages. Understanding the effects of different GFs on corneal wound healing will provide useful information for therapeutic purposes.

Acknowledgments

This work was supported by an FPI grant from Junta de Castilla y León - European Social Fund (Consejería de Educación, Spain). The authors wish to thank the Unidad de Apoyo a la Investigación/Hospital Clínico Universitario de Valladolid-IECSCYL for its technical support, Sagrario Callejo for her technical assistance with the confocal images and Mabel Cabero García for her technical assistance with the western blot techniques. Authors also acknowledge the assistance of Britt Bromberg, PhD, ELS of Xenofile Editing (www.xenofileediting.com) for the editing of the manuscript.

References

Anitua, E., de la Fuente, M., Muruzabal, F., Riestra, A., Merayo-Lloves, J., Orive, G., 2015. Plasma rich in growth factors (PRGF) eye drops stimulates scarless regeneration compared to autologous serum in the ocular surface stromal fibroblasts. Exp Eye Res 135, 118-126.

Bass, M.D., Roach, K.A., Morgan, M.R., Mostafavi-Pour, Z., Schoen, T., Muramatsu, T., Mayer, U., Ballestrem, C., Spatz, J.P., Humphries, M.J., 2007. Syndecan-4-dependent Rac1 regulation determines directional migration in response to the extracellular matrix. J Cell Biol 177, 527-538.

Bernstein, A.M., Greenberg, R.S., Taliana, L., Masur, S.K., 2004. Urokinase anchors uPAR to the actin cytoskeleton. Invest Ophthalmol Vis Sci 45, 2967-2977.

Birk, D.E., Fitch, J.M., Linsenmayer, T.F., 1986. Organization of collagen types I and V in the embryonic chicken cornea. Invest Ophthalmol Vis Sci 27, 1470-1477.

Boilly, B., Vercoutter-Edouart, A.S., Hondermarck, H., Nurcombe, V., Le Bourhis, X., 2000. FGF signals for cell proliferation and migration through different pathways. Cytokine Growth Factor Rev 11, 295-302.

Brooks, R., Williamson, R., Bass, M., 2012. Syndecan-4 independently regulates multiple small GTPases to promote fibroblast migration during wound healing. Small GTPases 3, 73-79.

Carey, D.J., 1997. Syndecans: multifunctional cell-surface co-receptors. Biochem J 327 (Pt 1), 1-16.

Carter, R.T., 2009. The role of integrins in corneal wound healing. Vet Ophthalmol 12 Suppl 1, 2-9.

Chen, C., Michelini-Norris, B., Stevens, S., Rowsey, J., Ren, X., Goldstein, M., Schultz, G., 2000. Measurement of mRNAs for TGFss and extracellular matrix proteins in corneas of rats after PRK. Invest Ophthalmol Vis Sci 41, 4108-4116.

Couchman, J.R., Woods, A., 1999. Syndecan-4 and integrins: combinatorial signaling in cell adhesion. J Cell Sci 112 (Pt 20), 3415-3420.

Etheredge, L., Kane, B.P., Hassell, J.R., 2009. The effect of growth factor signaling on keratocytes in vitro and its relationship to the phases of stromal wound repair. Invest Ophthalmol Vis Sci 50, 3128-3136.

Fini, M.E., 1999. Keratocyte and fibroblast phenotypes in the repairing cornea. Prog Retin Eye Res 18, 529-551.

Funderburgh, J.L., Funderburgh, M.L., Mann, M.M., Corpuz, L., Roth, M.R., 2001. Proteoglycan expression during transforming growth factor beta -induced keratocyte-myofibroblast transdifferentiation. J Biol Chem 276, 44173-44178.

Galiacy, S.D., Fournie, P., Massoudi, D., Ancele, E., Quintyn, J.C., Erraud, A., Raymond-Letron, I., Rolling, F., Malecaze, F., 2011. Matrix metalloproteinase 14 overexpression reduces corneal scarring. Gene Ther 18, 462-468.

Hahnel, C., Somodi, S., Weiss, D.G., Guthoff, R.F., 2000. The keratocyte network of human cornea: a three-dimensional study using confocal laser scanning fluorescence microscopy. Cornea 19, 185-193.

Hassell, J.R., Cintron, C., Kublin, C., Newsome, D.A., 1983. Proteoglycan changes during restoration of transparency in corneal scars. Arch Biochem Biophys 222, 362-369.

Hassell, J.R., Schrecengost, P.K., Rada, J.A., SundarRaj, N., Sossi, G., Thoft, R.A., 1992. Biosynthesis of stromal matrix proteoglycans and basement membrane components by human corneal fibroblasts. Invest Ophthalmol Vis Sci 33, 547-557.

Imanishi, J., Kamiyama, K., Iguchi, I., Kita, M., Sotozono, C., Kinoshita, S., 2000. Growth factors: importance in wound healing and maintenance of transparency of the cornea. Prog Retin Eye Res 19, 113-129.

Kay, E.P., Lee, M.S., Seong, G.J., Lee, Y.G., 1998. TGF-beta s stimulate cell proliferation via an autocrine production of FGF-2 in corneal stromal fibroblasts. Curr Eye Res 17, 286-293.

Kim, A., Lakshman, N., Karamichos, D., Petroll, W.M., 2010. Growth factor regulation of corneal keratocyte differentiation and migration in compressed collagen matrices. Invest Ophthalmol Vis Sci 51, 864-875.

Kim, W.J., Mohan, R.R., Mohan, R.R., Wilson, S.E., 1999. Effect of PDGF, IL-1alpha, and BMP2/4 on corneal fibroblast chemotaxis: expression of the platelet-derived growth factor system in the cornea. Invest Ophthalmol Vis Sci 40, 1364-1372.

Le Clainche, C., Carlier, M.F., 2008. Regulation of actin assembly associated with protrusion and adhesion in cell migration. Physiol Rev 88, 489-513.

Long, C.J., Roth, M.R., Tasheva, E.S., Funderburgh, M., Smit, R., Conrad, G.W., Funderburgh, J.L., 2000. Fibroblast growth factor-2 promotes keratan sulfate proteoglycan expression by keratocytes in vitro. J Biol Chem 275, 13918-13923.

Maguen, E., Rabinowitz, Y.S., Regev, L., Saghizadeh, M., Sasaki, T., Ljubimov, A.V., 2008. Alterations of extracellular matrix components and proteinases in human corneal buttons with INTACS for post-laser in situ keratomileusis keratectasia and keratoconus. Cornea 27, 565-573.

Maltseva, O., Folger, P., Zekaria, D., Petridou, S., Masur, S.K., 2001. Fibroblast growth factor reversal of the corneal myofibroblast phenotype. Invest Ophthalmol Vis Sci 42, 2490-2495.

Michelacci, Y.M., 2003. Collagens and proteoglycans of the corneal extracellular matrix. Braz J Med Biol Res 36, 1037-1046.

Mongiat, M., Taylor, K., Otto, J., Aho, S., Uitto, J., Whitelock, J.M., Iozzo, R.V., 2000. The protein core of the proteoglycan perlecan binds specifically to fibroblast growth factor-7. J Biol Chem 275, 7095-7100.

Petroll, W.M., Lakshman, N., Ma, L., 2012. Experimental Models for Investigating Intra-Stromal Migration of Corneal Keratocytes, Fibroblasts and Myofibroblasts. J Funct Biomater 3, 183-198.

Rawe, I.M., Meek, K.M., Leonard, D.W., Takahashi, T., Cintron, C., 1994. Structure of corneal scar tissue: an X-ray diffraction study. Biophys J 67, 1743-1748.

Singh, V., Agrawal, V., Santhiago, M.R., Wilson, S.E., 2012. Stromal fibroblast-bone marrow-derived cell interactions: Implications for myofibroblast development in the cornea. Exp Eye Res 98, 1-8.

Singh, V., Santhiago, M.R., Barbosa, F.L., Agrawal, V., Singh, N., Ambati, B.K., Wilson, S.E., 2011. Effect of TGFbeta and PDGF-B blockade on corneal myofibroblast development in mice. Exp Eye Res 93, 810-817.

Sloniecka, M., Le Roux, S., Zhou, Q., Danielson, P., 2016. Substance P Enhances Keratocyte Migration and Neutrophil Recruitment through Interleukin-8. Mol Pharmacol 89, 215-225.

Song, Q.H., Klepeis, V.E., Nugent, M.A., Trinkaus-Randall, V., 2002. TGF-beta1 regulates TGF-beta1 and FGF-2 mRNA expression during fibroblast wound healing. Mol Pathol 55, 164-176.

Stepp, M.A., 2006. Corneal integrins and their functions. Exp Eye Res 83, 3-15.

Sundarraj, N., Fite, D., Belak, R., Sundarraj, S., Rada, J., Okamoto, S., Hassell, J., 1998. Proteoglycan distribution during healing of corneal stromal wounds in chick. Exp Eye Res 67, 433-442.

Torricelli, A.A., Marino, G.K., Santhanam, A., Wu, J., Singh, A., Wilson, S.E., 2015. Epithelial basement membrane proteins perlecan and nidogen-2 are up-regulated in stromal cells after epithelial injury in human corneas. Exp Eye Res 134, 33-38.

Torricelli, A.A., Singh, V., Agrawal, V., Santhiago, M.R., Wilson, S.E., 2013. Transmission electron microscopy analysis of epithelial basement membrane repair in rabbit corneas with haze. Invest Ophthalmol Vis Sci 54, 4026-4033.

Tuli, S.S., Liu, R., Chen, C., Blalock, T.D., Goldstein, M., Schultz, G.S., 2006. Immunohistochemical localization of EGF, TGF-alpha, TGF-beta, and their receptors in rat corneas during healing of excimer laser ablation. Curr Eye Res 31, 709-719.

Wang, L., Ko, C.Y., Meyers, E.E., Pedroja, B.S., Pelaez, N., Bernstein, A.M., 2011. Concentration-dependent effects of transforming growth factor beta1 on corneal wound healing. Mol Vis 17, 2835-2846.

West-Mays, J.A., Dwivedi, D.J., 2006. The keratocyte: corneal stromal cell with variable repair phenotypes. Int J Biochem Cell Biol 38, 1625-1631.

Wilson, S.E., Mohan, R.R., Mohan, R.R., Ambrosio, R., Jr., Hong, J., Lee, J., 2001. The corneal wound healing response: cytokine-mediated interaction of the epithelium, stroma, and inflammatory cells. Prog Retin Eye Res 20, 625-637.

Wilson, S.E., Schultz, G.S., Chegini, N., Weng, J., He, Y.G., 1994. Epidermal growth factor, transforming growth factor alpha, transforming growth factor beta, acidic fibroblast growth factor, basic fibroblast growth factor, and interleukin-1 proteins in the cornea. Exp Eye Res 59, 63-71.

Woods, A., Couchman, J.R., 1994. Syndecan 4 heparan sulfate proteoglycan is a selectively enriched and widespread focal adhesion component. Mol Biol Cell 5, 183-192.

Zaidel-Bar, R., Ballestrem, C., Kam, Z., Geiger, B., 2003. Early molecular events in the assembly of matrix adhesions at the leading edge of migrating cells. J Cell Sci 116, 4605-4613.

Table 1. Effect of GF treatment on wound widths

	Wound widths*			
Treatment	Day 0	Day 4	Day 10	Day 15
SFM	768.50±65.87 μm	365.45±63.08 μm†	83.51±10.49 μm#	0±0 μm
TGFβ1		255.50±44.07 μm‡	98.80±12.52 μm	84.38±11.79 μm
PDGF-BB		172.85±25.43 μm§	0±0 μm	
bFGF		171.71±25.15 μmǁ	0±0 μm	

SFM, serum free medium; TGFβ1, transforming growth factor β1; PDGF-BB, dimeric B-chain platelet derived growth factor; bFGF, basic fibroblast growth factor. *, all values refer to the width of the wound. †, ‡, § and ǁ denote statistically significant differences at $p<0.001$ level on Day 4. # denote statistically significant differences at $p<0.01$ level on Day 10.
† SFM: vs TGFβ1; vs PDGF-BB; vs bFGF.
‡ TGFβ1: vs SFM; vs bFGF; vs PDGF-BB.
§ PDGF-BB: vs SFM; vs TGFβ1.
ǁ bFGF: vs SFM; vs TGFβ1.
#SFM vs TGFβ1.

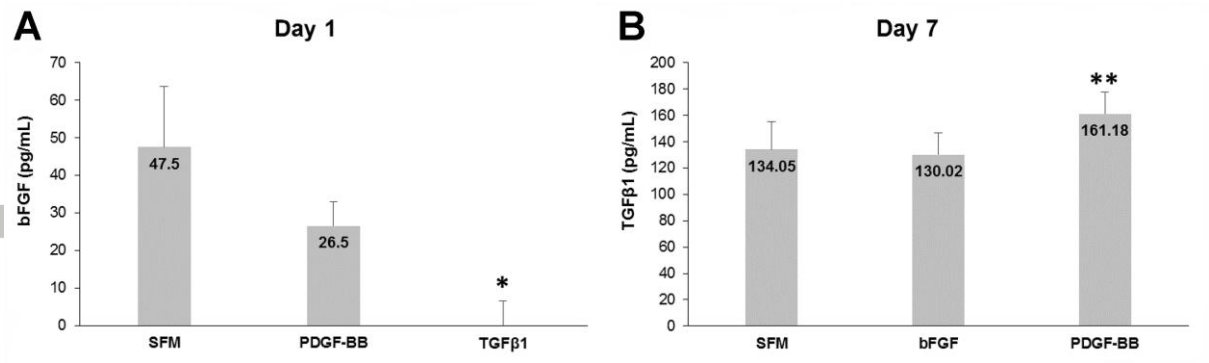

Figure 1. Detection of bFGF and TGFβ1. The quantities of both GFs secreted into the culture media by HCFs were compared among treatments on Days 1 and 7 after wounding. (A) bFGF detected at Day 1 after wounding. (B)TGFβ1 detected at Day 7 after wounding. *p< 0.05; **p< 0.01.

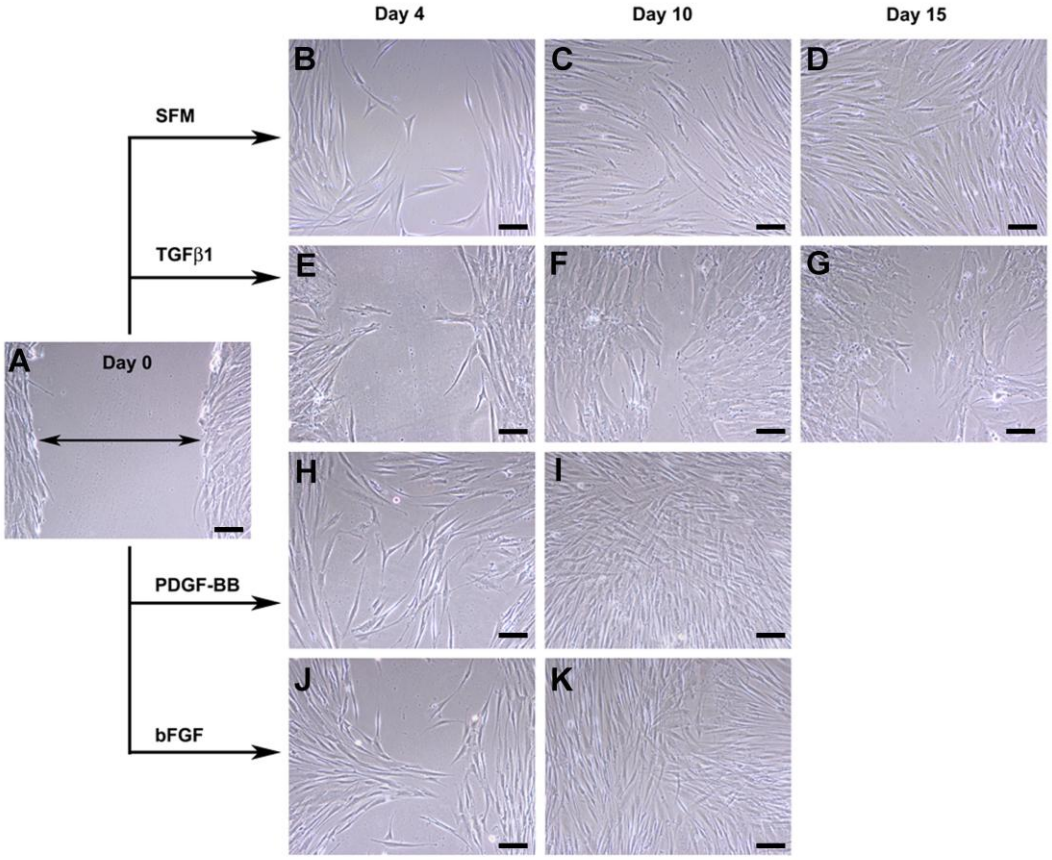

Figure 2. Wound closure (A-K). The representative micrographs show wound closure in HCFs cultured in SFM (B-D) or SFM supplemented with TGFβ1 (E-G), PDGF-BB (H-I), or bFGF (J-K) at 0, 4, 10, and 15 days after wounding until wound closure was complete. 100x magnification, scale bars 100 µm.

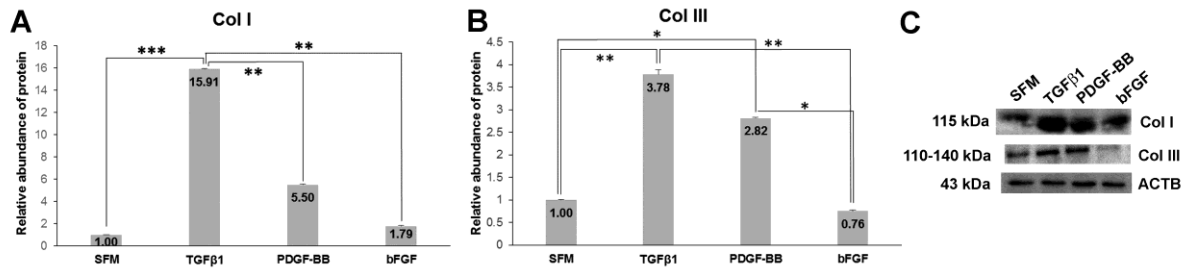

Figure 3. Relative abundance of Col I and Col III proteins. Relative changes in the abundance of each protein were compared among treatments at Day 7 after wounding. (A) Col I. (B) Col III. All results are presented relative to the SFM sample normalized to 1. *p<0.05; **p<0.01; ***p<0.001. (C) Immunoblotting analysis showing expression of Col I (115 kDa) and Col III (110-140 kDa). As a loading control, ACTB was detected as a 43 kDa band.

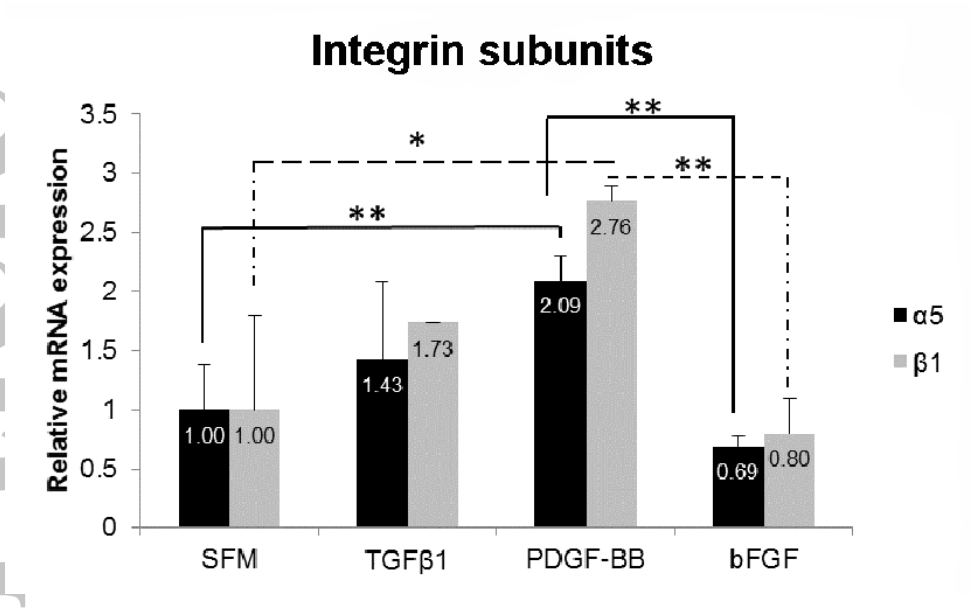

Figure 4. Relative mRNA expression levels for α5 and β1-integrin subunits. Relative changes in gene transcription were compared among treatments at Day 7 after wounding. Results are presented relative to the SFM sample normalized to 1. *p<0.05; **p<0.01.

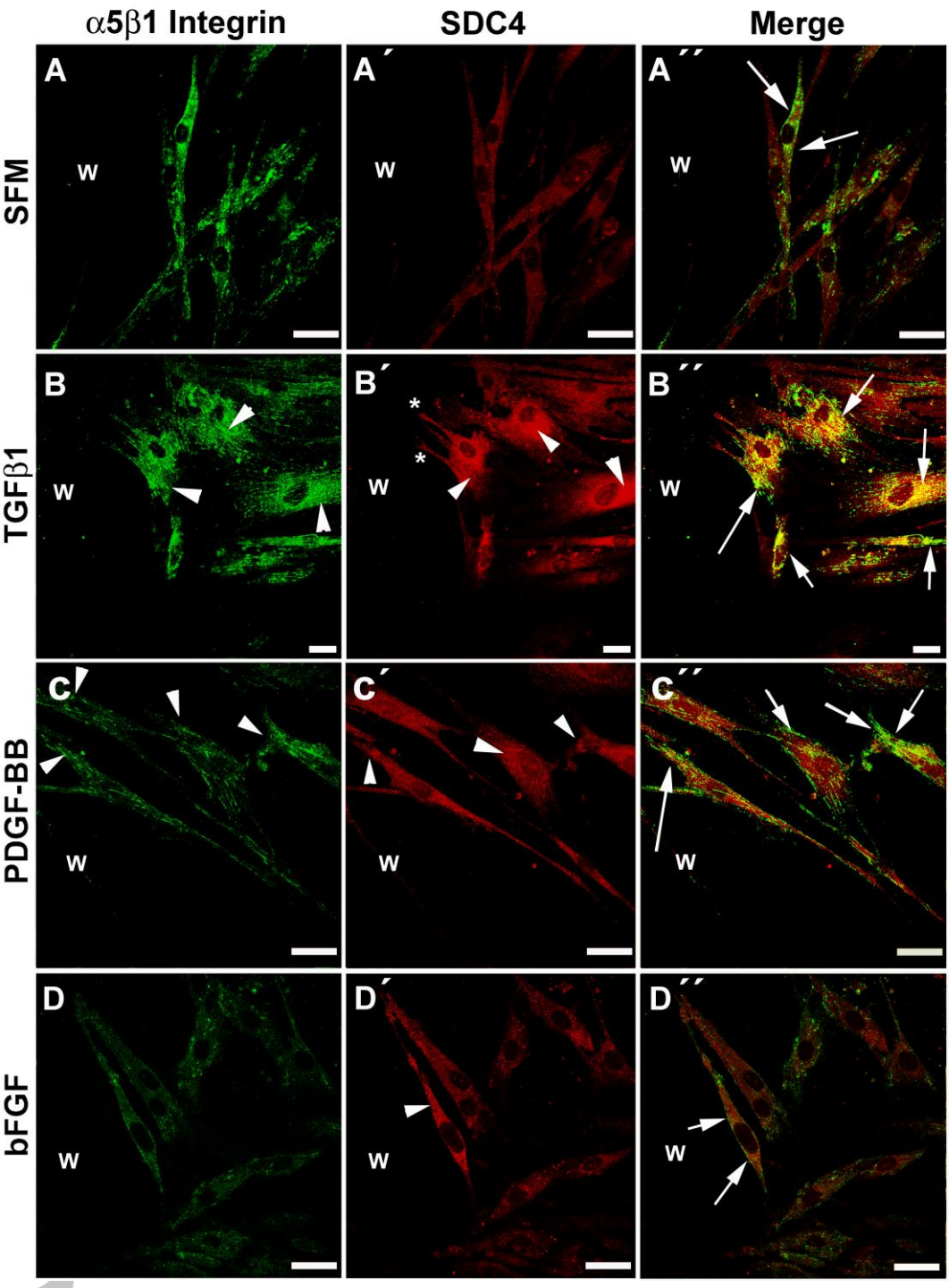

Figure 5. HCFs treated with different GFs at Day 4 after wounding, and co-immunostained with target-specific antibodies against α5β1 integrin (A-D) and the SDC4 (A´-D´). In these representative photomicrographs, W shows the wound area; arrowheads indicate protein accumulation sites in the cells; asterisks show protein localization in filopodia. The last column shows the merged images of the SDC4 and α5β1 integrin (A´´-D´´); arrows indicate α5β1 integrin and the SDC4 co-localization in the cells; scale bars 25 μm.

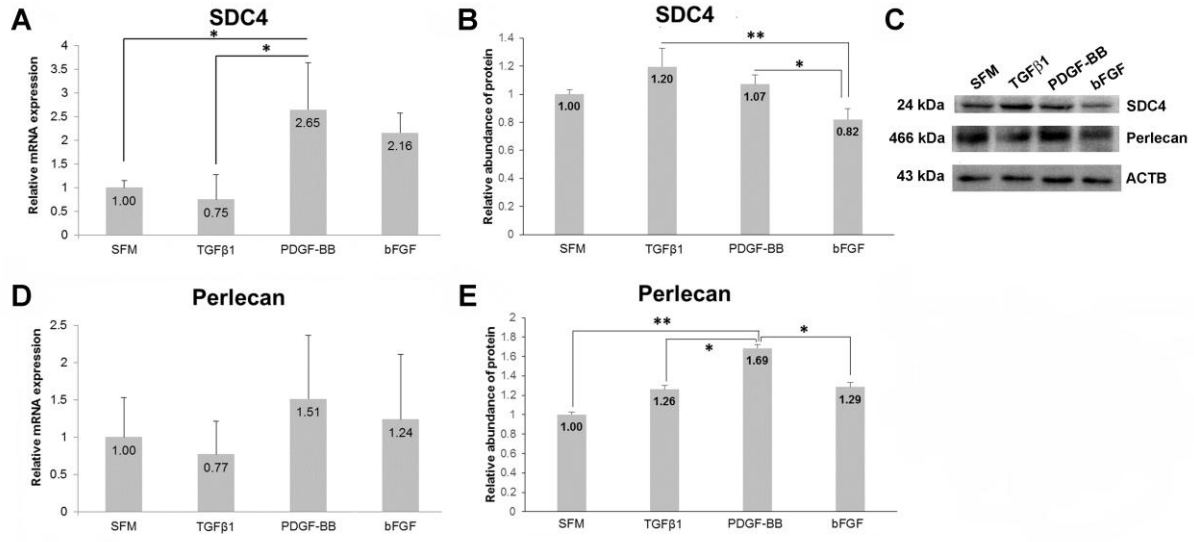

Figure 6. Relative mRNA expression and relative abundance of the SDC4 and perlecan proteins. Relative changes in mRNA expression and abundance of each protein were compared among treatments at Day 7 after wounding. (A, B) SDC4. (D, E) Perlecan. All results are presented relative to the SFM sample normalized to 1. *p<0.05; **p<0.01. (C) Immunoblotting analysis showing expression of SDC4 (24 kDa) and Perlecan (466 kDa). As a loading control, ACTB was detected as a 43 kDa band.